

CHEMISTRY

A European Journal

A Journal of



Accepted Article

Title: Surface Deactivated Core-Shell Metal-Organic Framework by Simple Ligand Exchange for Enhanced Size Discrimination in Aerobic Oxidation of Alcohols

Authors: Seongwoo Kim, Jooyeon Lee, Sungeun Jeoung, Hoi Ri Moon, and Min Kim

This manuscript has been accepted after peer review and appears as an Accepted Article online prior to editing, proofing, and formal publication of the final Version of Record (VoR). This work is currently citable by using the Digital Object Identifier (DOI) given below. The VoR will be published online in Early View as soon as possible and may be different to this Accepted Article as a result of editing. Readers should obtain the VoR from the journal website shown below when it is published to ensure accuracy of information. The authors are responsible for the content of this Accepted Article.

To be cited as: *Chem. Eur. J.* 10.1002/chem.202000933

Link to VoR: <http://dx.doi.org/10.1002/chem.202000933>

Supported by
ACES

WILEY-VCH

COMMUNICATION

Surface Deactivated Core-Shell Metal-Organic Framework by Simple Ligand Exchange for Enhanced Size Discrimination in Aerobic Oxidation of Alcohols

Seongwoo Kim,^[a] Jooyeon Lee,^{[a][†]} Sungeun Jeoung,^{[b][†]} Hoi Ri Moon,^{*[b]} and Min Kim^{*[a]}

[†] These authors equally contributed to this work.

[a] S. Kim, J. Lee,^[†] Prof. Dr. M. Kim*
Department of Chemistry and BK21Plus Research Team
Chungbuk National University
Cheongju 28644, Republic of Korea
E-mail: minkim@chungbuk.ac.kr

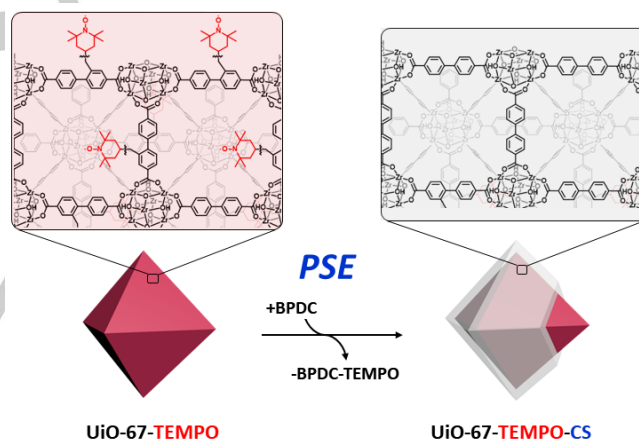
[b] Dr. S. Jeoung,^[†] Prof. Dr. H. R. Moon*
Department of Chemistry
Ulsan National Institute of Science and Technology
Ulsan 44919, Republic of Korea
E-mail: hoirimoon@unist.ac.kr

Supporting information for this article is given via a link at the end of the document.

Abstract: Metal-organic frameworks (MOFs) are the attractive catalyst support for stable immobilization of the active sites in their scaffold due to its high tunability of organic ligands. The active site-functionalized ligands can be easily employed to construct MOFs as porous heterogeneous catalysts. However, the existence of active sites on the external surfaces as well as internal pores of MOFs seriously impedes the selective reaction in the pore. Herein, via a simple postsynthetic ligand exchange (PSE) method we synthesized the surface deactivated (only pore-active) core-shell type-MOF catalysts, which contain 2,2,6,6-tetramethylpiperidin-1-yl)oxyl (TEMPO) groups on the ligand as active sites for aerobic oxidation of alcohols. The porous but catalytically inactive shell ensured the size-selective permeability by sieving effects and induced all reactions to take place in the pore of catalytically active core. Because PSE is the facile and universal approach, this can be rapidly applied to a variety of MOF-based catalysts for enhancing reaction selectivity.

A large degree of tunability in building blocks for metal-organic frameworks (MOFs) construction enables facile pore engineering.^[1] Well-tailored pore size and structures in MOFs grant the functions of molecular sieve to be applicable to gas storage, molecular separation, and catalysis.^[2] For the utilization of MOFs as catalysts, their well-defined pore structure, which is the key factor for the size-selective nanoreactor, attracted great attention for many important reactions.^[3] Furthermore, since organic ligands for MOF construction can be widely substituted by target functional groups, the immobilization of the catalytically active sites on their scaffold via covalent bonds enable to develop the stable heterogeneous catalysts, which efficiently alleviate the reduction of catalytic performance during the reaction.^[4] Owing to these merits of MOFs, efficient and size-selective catalytic reaction in MOFs have been intensively studied.^[5] However, size-selective reaction by the MOF catalysts should be carefully analyzed and discussed. If the catalytic reaction is fast and substrate diffusion into the pores is slow, the majority of the reaction will occur on the surface of the catalyst, not inside the pores.^[6] To achieve good size selectivity, it should be sure to

restrict the presence of the active sites on the external surface and make sure that all reactions take place in the confined pore space.



Scheme 1. Schematic illustration of TEMPO-functionalized UiO-67 (UiO-67-TEMPO) and the surface deactivated core-shell type MOF catalyst (UiO-67-TEMPO-CS) obtained via postsynthetic ligand exchange with non-functionalized BPDC ligand.

Postsynthetic ligand exchange (PSE) is the simple but versatile strategy to modify functionality of as-synthesized MOFs.^[7] Since the coordination between the metal in the SBU (secondary building unit) and the ligand of MOF is in equilibrium, the original ligands in the MOFs are exchanged with new ligands by soaking MOF crystals in the pure ligand solution. In addition, upon varying the amount of ligand used in PSE, the extent of ligand exchange can be controlled. Previously, the various factors of PSE such as concentration, solvent, temperature and time have been intensively studied.^[7b,d] Especially, Matzger *et al* examined the microstructure of MOFs after PSE for carboxylic acid ligands, which reveal that the exchanged ligand is mainly

COMMUNICATION

located at the edges of the crystal, resulting in the core-shell structure.^[8] Due to the slow diffusion of the carboxylic acid ligand into the pores, ligand exchange from the surface of MOFs occurs faster than diffusion into the pores. This provides the wide opportunities to modify the exterior of MOF crystals, and in the present study, we employed this method to deactivate the surface of MOF catalysts. Herein, we selected the zirconium-based MOF, UiO-67 system (UiO = University of Oslo) as the catalyst support to anchor 2,2,6,6-tetramethylpiperidin-1-yl)oxyl (TEMPO) groups as an active site for aerobic oxidation of alcohols, yielding the catalyst, UiO-67-TEMPO. By the PSE treatment of UiO-67-TEMPO, the surface-deactivated core-shell type MOF catalyst, UiO-67-TEMPO-CS was successfully prepared (Scheme 1). Only pore-active MOF catalysts exhibited the high size-selective reactivity for aerobic oxidation of alcohols, which contrasts with low selectivity of the untreated UiO-67-TEMPO.

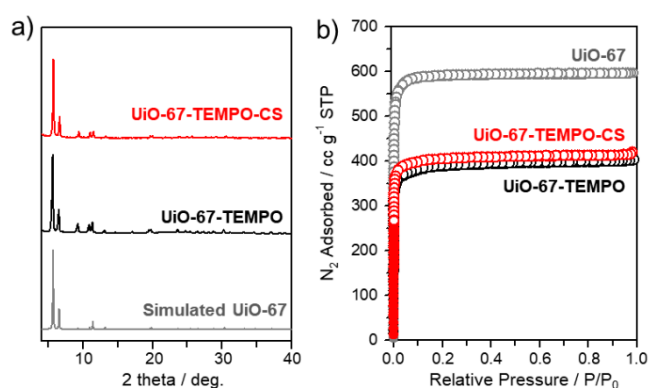


Figure 1. a) PXRD patterns and b) N_2 full isotherms of UiO-67-TEMPO and UiO-67-TEMPO-CS.

A parent MOF catalyst, UiO-67-TEMPO, was prepared from the solvothermal reaction with $ZrCl_4$ and the mixture ligand system of biphenyl-4,4'-dicarboxylic acid (BPDC) and BPDC-TEMPO (1:1 in mole ratio) in acidic condition. The resultant colorless microcrystals have the identical structure with UiO-67, confirmed by the powder X-ray diffraction pattern (PXRD, Figure 1a). It is composed of BPDC and BPDC-TEMPO in 55:45 of mole ratio as evidenced by 1H NMR, which was measured with the solution of acidic digestion (Figure S1). In order to achieve the surface deactivated MOF catalyst (UiO-67-TEMPO-CS), UiO-67-TEMPO was incubated in the solution containing 0.75 equivalents of the pure BPDC ligand at 35 °C for 18 h with shaking. As compared in Figure 1a, after this PSE process the structure of collected solids were well-retained, and the ratio between BPDC and BPDC-TEMPO was significantly changed to 76:24 (Figure S2). As previously studied, the PSE ratio (e.g., BPDC : BPDC-TEMPO) is directly related with the amount of structural defects in MOFs.^[7d] Therefore, all pristine UiO-67-TEMPO materials were prepared by identical solvothermal condition and acid modulator. To understand the pore structure of MOFs before and after PSE treatment, we conducted N_2 adsorption/desorption experiments at 77 K for UiO-67, UiO-67-TEMPO and UiO-67-TEMPO-CS. Compared with UiO-67, UiO-67-TEMPO, in which a half of BPDC is replaced by BPDC-TEMPO, shows the reduced Brunauer-Emmett-Teller (BET) surface area from 2208 to 1169 m^2/g , attributed to the bulkiness of TEMPO groups. The BET surface

area of exchanged UiO-67-TEMPO-CS were 1218 m^2/g , slightly larger than that of the parent compound (Figure 1b).

Although the degree of ligand exchange by postsynthetic modification was quantitatively analyzed by 1H NMR, the study of the exchanged ligand position in UiO-67-TEMPO-CS is essential to confirm the formation of the core-shell structure. Since the parent UiO-67-TEMPO also contained BPDC ligand in the framework, the position of the exchanged BPDC ligand in UiO-67-TEMPO-CS is indistinguishable from the former one. Thus, as following the recent method reported by Matzger's group, PSE was conducted with deuterated BPDC- d_8 ligand, in which asymmetric C-C stretch mode of BPDC- d_8 are clearly distinguishable from that of BPDC by Raman spectroscopy.^[8] Unfortunately, deuterated BPDC- d_8 is not commercially available; therefore, partially deuterated BPDC- d_8 (30% d -incorporated for 2,2'-positions and 90% d -incorporated for 3,3'-positions) was synthesized in multiple steps (see the Supporting Information for details, Scheme S2 and Figure S3). UiO-67-TEMPO-CS(D) was obtained from PSE of UiO-67-TEMPO with BPDC- d_8 in same PSE condition of UiO-67-TEMPO-CS. In order to examine the microstructure of UiO-67-TEMPO-CS(D), its single crystal was sectioned in an epoxy resin and its cross section was analyzed by mapping with a Raman microscope (Figure 2a). In the point Raman spectrum of the core part of the UiO-67-TEMPO-CS(D) (Figure 2b), one large peak at centered 1611 cm^{-1} was observed, which is assigned as asymmetric C-C stretching mode of the phenyl rings in BPDC. However, at the outer shell of the UiO-67-TEMPO-CS(D) the additional band appeared at 1583 cm^{-1} , which is corresponded to the same vibrational mode from deuterated BPDC- d_8 .^[9] Based on this result, we confirm the ligand exchange of UiO-67-TEMPO occurred mainly from the surface of the crystals, forming the core-shell structure. It implies that simple PSE treatment successfully deactivate the surface of UiO-67-TEMPO by catalytically inactive BPDC without loss of crystallinity as well as textural properties (Figures 1 and S4). The surface-deactivated core-shell MOFs could also be obtained by different strategical approach, overgrowth methods.^[10]

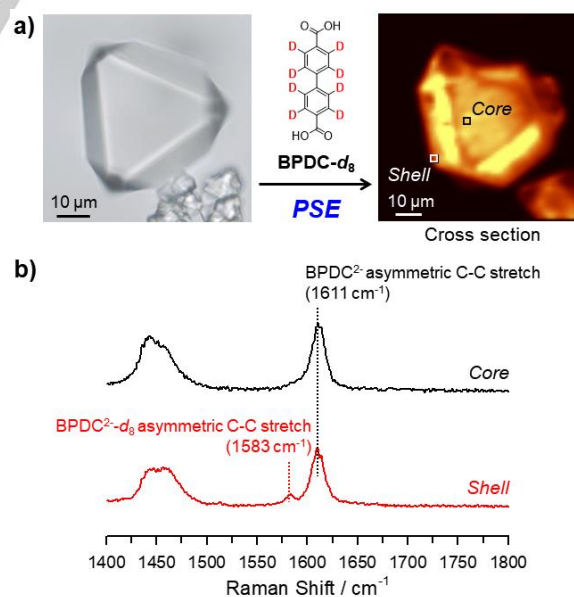


Figure 2. (a) The optical microscopic image of UiO-67-TEMPO and Raman mapping of cross-sectioned core-shell type MOF via postsynthetic BPDC- d_8 ligand exchange (UiO-67-TEMPO-CS(D)). (b) Point Raman spectra of UiO-67-TEMPO-CS(D), which were obtained from the positions indicated in (a).

COMMUNICATION

The catalytic reactivity of UiO-67-TEMPO was examined for aerobic oxidation of alcohols with a variety of substrates under various conditions.^[11] In this study, we additionally used $\text{Eu}(\text{NO}_3)_3$ as a metal catalyst with TEMPO-immobilized MOFs, in which the combinational catalysts can show the enhanced performance based on the previous studies in homogeneous catalysts. Transition metal-TEMPO-catalyzed aerobic oxidation generally has three cooperative redox cycles: the redox cycle of the metal cations, the cycle of the external oxidant (such as TEMPO), and the O_2 -water-related cycle (Scheme S3).^[12] Thus, the combination of metal catalyst and TEMPO generally shows higher reaction efficiency and wider substrate scopes than organic oxidant-only systems. In addition, recently the redox cycle of $\text{Eu}(\text{II})/\text{Eu}(\text{III})$ have been successfully applied to the aerobic oxidation under mild condition with similar proposed mechanism.^[13] Accordingly, to adopt this catalytic system to heterogeneous catalyst, UiO-67-TEMPO with europium nitrate was used for aerobic oxidation with a variety of aldehydes with different size in the present study (Figure 3, Tables S1 and S2). To the best of our knowledge, this is the first attempt to utilize the combination system of metal catalysts and TEMPO species for aerobic oxidation by MOF-catalysis, although the previously reported TEMPO only-functionalized MOFs were successfully demonstrated in the aerobic oxidation of alcohols.^[5d, 11] The experiments conducted with different catalyst combinations for benzyl alcohol (**1a**) oxidation clearly showed that the simultaneous use of UiO-67-TEMPO and $\text{Eu}(\text{NO}_3)_3$ exhibited 97% conversion to benzaldehyde (**2a**), which is the comparable result from homogeneous reaction of $\text{Eu}(\text{NO}_3)_3$ and TEMPO (entries 3 and 4 in Table S1). In addition, UiO-67-TEMPO could be recycled up to three times by simple centrifugation. There is no significant decrease of reactivity in the second run. In the third run, the conversion for aerobic oxidation was slightly decreased and partial amorphization was observed in the PXRD pattern of recovered UiO-67-TEMPO (Figure S5). Under the optimized reaction condition (Condition A: 1 mol% of UiO-67-TEMPO and 1 mol% of $\text{Eu}(\text{NO}_3)_3$ at 60 °C for 9 h), benzyl alcohol (**1a**) and diphenyl methanol (**1b**) were fully converted to benzaldehyde (**2a**, 99%) and diphenyl ketone (**2b**, 99%), showing good reactivity for primary and secondary alcohols (Figure 3 and Table S2). In addition, a series of alcohol substrates with electron-donating groups and electron-withdrawing groups (entries 5-7 in Table S2) as well as *ortho*-, *meta*-, and *para*-substituted primary alcohols (entries 7-9 and 11-13 in Table S2) were successfully converted to the aldehydes with good conversions. However, bulky substrates such as pyrenyl methanol and phenyl pyrenyl methanol (**1c** and **1d**) showed relatively lower reactivity with UiO-67-TEMPO (45% for **2c** and 38% for **2d**, Figure 3 and Table S2), but the conversions were significant enough, showing low size-selectivity.

In order to test the surface deactivation effect of the MOF catalyst on the size selectivity, the catalytic reactivity of UiO-67-TEMPO-CS was compared with that of UiO-67-TEMPO (Figure 3 and Table S3). The overall reactivity of UiO-67-TEMPO-CS was lower than that of UiO-67-TEMPO; thus, 5 mol% catalyst loading (Condition B: 5 mol% for each $\text{Eu}(\text{NO}_3)_3$, UiO-67-TEMPO-CS, and NaNO_3) and longer reaction time (18 h) were employed to obtain full conversion in the oxidation of benzyl alcohol (**1a**) to benzaldehyde (**2a**). In accord with our hypothesis, effective size discrimination was demonstrated by these surface-deactivated UiO-67-TEMPO-CS, as the smallest substrates (benzyl alcohol

(**1a**) and diphenyl methanol (**1b**) showed full conversions under the optimized conditions, and pyrenyl methanol (**1c**), a larger substrate, showed poor conversion (17%), and phenyl pyrenyl methanol (**1d**) showed almost no reactivity even when increasing the reaction time (Figure 3 and Table S3). In addition, similar catalytic behaviors of UiO-67-TEMPO and UiO-67-TEMPO-CS for small substrates (both **1a** and **1b**) were confirmed by kinetic curves against reaction time (Figure S6).

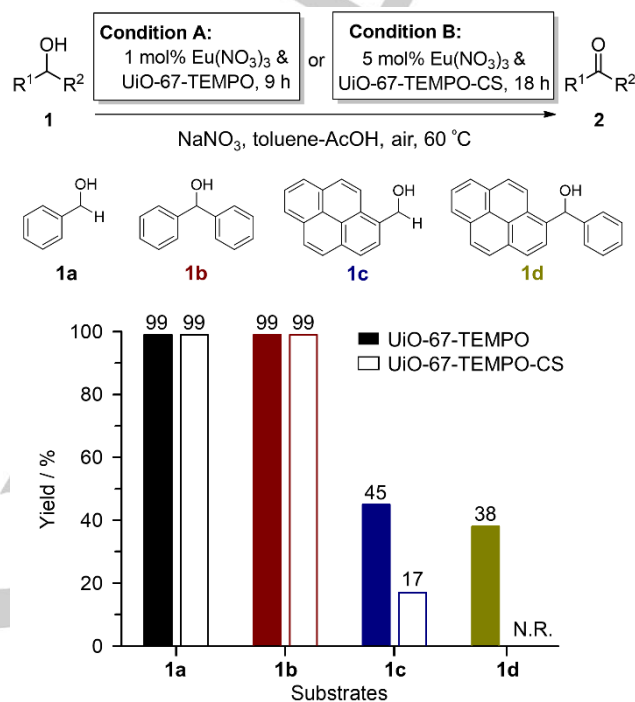


Figure 3. Size Discrimination on Aerobic Oxidation of Alcohols with UiO-67-TEMPO (Condition A) and UiO-67-TEMPO-CS (Condition B).

The molecular sizes of starting alcohols were simply calculated through B3LYP/6-311G (Figure S7), and comparison of molecular sizes with NLDFT pore size distribution analysis confirmed the diffusion difficulty of phenyl pyrenyl methanol (**1d**) to MOF pores (Figure S8). Once again, from the pristine UiO-67-TEMPO (*i.e.*, surface active), the exposed TEMPO residue in the MOF surface could perform the aerobic oxidation of alcohols; thus, moderate conversion was observed for phenyl pyrenyl methanol (**1d**), the largest substrate tested of Figure 3. In contrast, the surface deactivate UiO-67-TEMPO-CS showed no efficiency for the aerobic oxidation of phenyl pyrenyl methanol (**1d**).

Table 1: Size discrimination from the substrate mixtures in the aerobic oxidation.^[a]

Entry	TEMPO species	Yield (%) of 2a ^[b]	Yield (%) of 2d ^[b]
1	UiO-67-TEMPO-CS	91	N.R.

COMMUNICATION

2	UiO-67-TEMPO	93	68
3	TEMPO	96	85

[a] Benzyl alcohol (**1a**, 27 mg, 0.25 mmol), phenyl pyrenyl methanol (**1d**, 27 mg, 0.088 mmol), $\text{Eu}(\text{NO}_3)_3$ (0.0063 mmol), TEMPO species (0.0063 mmol), and NaNO_3 (1 mg, 0.0063 mmol) in a solvent mixture of toluene (3 mL) and AcOH (0.05 mL) at 60 °C for 18 h. [b] Isolation yield.

Furthermore, the starting material mixture was tested to confirm the size discrimination and reactivity differences between substrates. When using a mixture of benzyl alcohol (**1a**-smallest substrate) and phenyl pyrenyl methanol (**1d**-largest substrate) as the starting material, only conversion to benzaldehyde (**2a**) was observed, and phenyl pyrenyl ketone (**2d**, phenyl(pyren-1-yl)methanone) was not detected with this UiO-67-TEMPO-CS (entry 1 in Table 1, 1:1 wt% ratio was used for molecular size differences, see supporting information for detail). On the other hand, pristine UiO-67-TEMPO (non-PSE-treated, surface-active) did not show the size discrimination from the substrate mixtures (**1a** + **1d**, entry 2). Not surprisingly, the homogeneous system ($\text{Eu}(\text{NO}_3)_3$ + TEMPO molecule, entry 3) displayed totally non-selective conversion for the reagent mixture. In addition, it is clearly confirmed that the reactivity of **1a** and **1d** toward aerobic oxidation are similar (96% vs. 85%, entry 3). Therefore, the successful size discriminations from the substrate mixtures were only achieved with surface-deactivated core-shell type MOF catalyst, UiO-67-TEMPO-CS. Although PSE technique in MOFs have been utilized for installing the additional functionalities into the original structure in several reports,^[14] to the best of our knowledge, this is the first example of the deactivation of a MOF through the simple ligand exchange to achieve enhanced size discrimination. Moreover, since PSE is a universal and versatile method applicable to various MOFs and related systems, this methodology will impact multiple size-based properties of MOFs and their concomitant applications.

In conclusion, a simple PSE technique was adopted to deactivate the surface of the catalysts with UiO-67-TEMPO. The target aerobic oxidation of alcohols to corresponding aldehydes were successfully achieved by the combination of europium cation and TEMPO-functionalized MOFs with a wide range of functional group tolerance on the substrate. Surface deactivation through PSE with catalytically non-active ligand, BPDC, was performed on the UiO-67-TEMPO. Although PSE is a versatile and universal tool for MOF functionalization, to the best of our knowledge, this was the first attempt at deactivation of MOF through PSE. The core-shell structure and surface deactivation were confirmed by Raman spectra. Surprisingly, the surface-deactivated core-shell type MOF, UiO-67-TEMPO-CS, displayed excellent size discrimination based on the tested alcohols, and their resolution from a mixture of alcohols was achieved. This simple surface deactivation process provides an important and unique technique for tuning MOF catalysts and provides a route for novel, multifunctional MOF-based catalytic materials.

Acknowledgements

This work was supported by the Basic Science Research Program (2019R1A2C4070584) and the Science Research Center (2016R1A5A1009405) through the National Research Foundation of Korea (NRF) funded by the Ministry of Science and

ICT. S. Kim and J. Lee were supported by NRF Global Ph.D. Fellowship program (S. Kim for 2018H1A2A1062013; J. Lee for 2019H1A2A1076014) funded by the Ministry of Education.

Keywords: metal-organic framework, postsynthetic modification, ligand exchange, TEMPO, aerobic oxidation

- [1] a) Q. Wang, D. Astruc, *Chem. Rev.* **2019**, DOI 10.1021/acs.chemrev.9b00223; b) M. S. Denny, J. C. Moreton, L. Benz, S. M. Cohen, *Nat. Rev. Mater.* **2016**, *1*, 16078–16095; c) L. Li, L. Guo, Z. Zhang, Q. Yang, Y. Yang, Z. Bao, Q. Ren, J. Li, *J. Am. Chem. Soc.* **2019**, *141*, 9358–9364.
- [2] a) G. Liu, V. Chernikova, Y. Liu, K. Zhang, Y. Belmabkhout, O. Shekha, C. Zhang, S. Yi, M. Eddaoudi, W. J. Koros, *Nat. Mater.* **2018**, *17*, 283–289; b) G. Liu, A. Cadiau, Y. Liu, K. Adil, V. Chernikova, I.-D. Carja, Y. Belmabkhout, M. Karunakaran, O. Shekha, C. Zhang, A. K. Itta, S. Yi, M. Eddaoudi, W. J. Koros, *Angew. Chem. Int. Ed.* **2018**, *57*, 14811–14816; *Angew. Chem.* **2018**, *130*, 15027–15032; c) M. Jurcic, W. J. Peveler, C. N. Savory, D.-K. Bučar, A. J. Kenyon, D. O. Scanlon, I. P. Parkin, *ACS Appl. Mater. Interfaces* **2019**, *11*, 11618–11626; d) H. Wang, J. Li, *Acc. Chem. Res.* **2019**, *52*, 1968–1978; e) C. Satheeskumar, H. J. Yu, H. Par, M. Kim, J. S. Lee, M. Seo, *J. Mater. Chem. A* **2018**, *6*, 21961–21968; f) G. Huang, Q. Yang, Q. Xu, S. H. Yu, H. L. Jiang, *Angew. Chem. Int. Ed.* **2016**, *55*, 7379–7383; *Angew. Chem.* **2016**, *128*, 7505–7509; g) J.-R. Li, J. Sculley, H.-C. Zhou, *Chem. Rev.* **2012**, *112*, 869–932; h) B. Li, H. Wang, B. Chen, *Chem. Asian J.* **2014**, *9*, 1474–1498; i) Z. Kang, L. Fan, D. Sun, *J. Mater. Chem. A* **2017**, *5*, 10073–10091; j) S.-J. Lee, S. Kim, E.-J. Kim, M. Kim, Y.-S. Bae, *Chem. Eng. J.* **2018**, *335*, 345–351.
- [3] a) W. Lu, Z. Wei, Z. Y. Gu, T. F. Liu, J. Park, J. Park, J. Tian, M. Zhang, Q. Zhang, T. Gentle, et al., *Chem. Soc. Rev.* **2014**, *43*, 5561–5593; b) T. Drake, P. Ji, W. Lin, *Acc. Chem. Res.* **2018**, *51*, 2129–2138; c) Y. Wen, J. Zhang, Q. Xu, X.-T. Wu, Q.-L. Zhu, *Coord. Chem. Rev.* **2018**, *376*, 248–276; d) V. Pascanu, G. González Miera, A. K. Inge, B. Martin-Matute, *J. Am. Chem. Soc.* **2019**, *141*, 7223–7234.
- [4] a) D. Farrusseng, S. Aguado, C. Pinel, *Angew. Chem. Int. Ed.* **2009**, *48*, 7502–7513; *Angew. Chem.* **2009**, *121*, 7638–7649; b) A. Corma, H. Garcia, F. X. Llabres i Xamena, *Chem. Rev.* **2010**, *110*, 4606–4655; c) J. Gascon, A. Corma, F. Kapteijn, F. X. Llabres i Xamena, *ACS Catal.* **2014**, *4*, 361–378; d) J.-D. Xiao, H.-L. Jiang, *Acc. Chem. Res.* **2019**, *52*, 356–366; e) P. Hu, J. V. Morabito, C. K. Tsung, *ACS Catal.* **2014**, *4*, 4409–4419; f) T. Zhang, W. Lin, *Chem. Soc. Rev.* **2014**, *43*, 5982–5993; g) J. Liu, L. Chen, H. Cui, J. Zhang, L. Zhang, C. Y. Su, *Chem. Soc. Rev.* **2014**, *43*, 6011–6061; h) A. Dhakshinamoorthy, A. M. Asiri, H. Garcia, *Chem. Commun.* **2017**, *53*, 10851–10869; i) L. Zhu, X.-Q. Liu, H.-L. Jiang, L.-B. Sun, *Chem. Rev.* **2017**, *117*, 8129–8176; j) S. M. J. Rogge, A. Bavykina, J. Hajek, H. Garcia, A. I. Olivios-Suarez, A. Sepúlveda-Escribano, A. Vimont, G. Clet, P. Bazin, F. Kapteijn, et al., *Chem. Soc. Rev.* **2017**, *46*, 3134–3184.
- [5] a) P. Wu, C. He, J. Wang, X. Peng, X. Li, Y. An, C. Duan, *J. Am. Chem. Soc.* **2012**, *134*, 14991–14999; b) X.-L. Yang, M.-H. Xie, C. Zou, Y. He, B. Chen, M. O' Keeffe, C.-D. Wu, *J. Am. Chem. Soc.* **2012**, *134*, 10638–10645; c) S. Yuan, Y.-P. Chen, J.-S. Qin, W. Lu, L. Zou, Q. Zhang, X. Wang, X. Sun, H.-C. Zhou, *J. Am. Chem. Soc.* **2016**, *138*, 8912–8919; d) K. M. Zwołiński, M. J. Chmielewski, *ACS Appl. Mater. Interfaces* **2017**, *9*, 33956–33967; e) Y. Liu, J. Ma, P. Wu, J.-J. Zheng, X. Tian, M. Jiang, Y. He, H. Donga, J. Wang, *Dalton Trans.* **2019**, *48*, 11855–11861; f) Y. Zhong, Y. Mao, S. Shi, M. Wan, C. Ma, S. Wang, C. Chen, D. Zhao, N. Zhang, *ACS Appl. Mater. Interfaces* **2019**, *11*, 32251–32260; g) Y. Liu, Y. Shen, W. Zhang, J. Weng, M. Zhao, T. Zhu, Y. R. Chi, Y. Yang, H. Zhang, F. Huo, *Chem. Commun.* **2019**, *55*, 11770–11773.
- [6] J. Han, M. S. Lee, P. K. Thallapally, M. Kim, N. Jeong, *ACS Catal.* **2019**, *9*, 3969–3977.
- [7] a) M. Kim, J. F. Cahill, H. Fei, K. A. Prather, S. M. Cohen, *J. Am. Chem. Soc.* **2012**, *134*, 18082–18088; b) M. Kim, J. F. Cahill, Y. Su, K. A. Prather, S. M. Cohen, *Chem. Sci.* **2012**, *3*, 126–130; c) M. Bosch, S. Yuan, W. Rutledge, H. C. Zhou, *Acc. Chem. Res.* **2017**, *50*, 857–865; d) H.

COMMUNICATION

- Park, S. Kim, B. Jung, M. H. Park, Y. Kim, M. Kim, *Inorg. Chem.* **2018**, *57*, 1040–1047.
- [8] J. A. Boissonault, A. G. Wong-Foy, A. J. Matzger, *J. Am. Chem. Soc.* **2017**, *139*, 14841–14844.
- [9] a) A. Bree, C. Y. Pang, L. Rabeneck, *Spectrochim Acta* **1971**, *27A*, 1293–1298; b) W. Krasser, H. Ervens, A. Fadini, *J. Raman Spectrosc. Acta* **1980**, *9*, 80–84; c) Q. Zhou, Y. Yang, J. Ni, Z. Li, Z. Zhang, *Nano. Res.* **2010**, *3*, 423–428.
- [10] a) K. Hirai, S. Furukawa, M. Kondo, H. Uehara, O. Sakata, S. Kitagawa, *Angew. Chem. Int. Ed.* **2011**, *50*, 8057–8061; *Angew. Chem.* **2011**, *123*, 8207–8211; b) S. Choi, T. Kim, H. Ji, H. J. Lee, M. Oh, *J. Am. Chem. Soc.* **2016**, *138*, 14434–14440; c) F. Wang, S. He, H. Wang, S. Zhang, C. Wu, H. Huang, Y. Pang, C.-K. Tsung, T. Li, *Chem. Sci.* **2019**, *10*, 7755–7761.
- [11] a) Z. Li, T. Liu, X. Kang, Y. Cui, *Inorg. Chem.* **2018**, *57*, 9786–9789; b) L. Yang, L. Cao, R. Huang, Z. W. Hou, X. Y. Qian, B. An, H. C. Xu, W. Lin, C. Wang, *ACS Appl. Mater. Interfaces* **2018**, *10*, 36290–36296; c) A. Dhakshinamoorthy, M. Alvaro, H. Garcia, *ACS Catal.* **2011**, *1*, 48–53; d) L. Li, R. Matsuda, I. Tanaka, H. Sato, P. Kanoo, H. J. Jeon, M. L. Foo, A. Wakamiya, Y. Murata, S. Kitagawa, *J. Am. Chem. Soc.* **2014**, *136*, 7543–7546; e) J. L. Zhuang, X. Y. Liu, Y. Zhang, C. Wang, H. L. Mao, J. Guo, X. Du, S. Bin Zhu, B. Ren, A. Terfort, *ACS Appl. Mater. Interfaces* **2019**, *11*, 3034–3043.
- [12] a) J. M. Hoover, B. L. Ryland, S. S. Stahl, *J. Am. Chem. Soc.* **2013**, *135*, 2357–2367; b) S. Ma, J. Liu, S. Li, B. Chen, J. Cheng, J. Kuang, Y. Liu, B. Wan, Y. Wang, J. Ye, et al., *Adv. Synth. Catal.* **2011**, *353*, 1005–1017; c) K. Lagerblom, J. Keskiaväli, A. Parviainen, J. Mannisto, T. Repo, *ChemCatChem* **2018**, *10*, 2908–2914.
- [13] S. Kim, Y. Kim, H. Jin, M. H. Park, Y. Kim, K. M. Lee, M. Kim, *Adv. Synth. Catal.* **2019**, *361*, 1259–1264.
- [14] a) C. Tan, X. Han, Z. Li, Y. Liu, Y. Cui, *J. Am. Chem. Soc.* **2018**, *140*, 16229–16236; b) X. Zhang, J. Sun, G. Wei, Z. Liu, H. Yang, K. Wang, H. Fei, *Angew. Chem. Int. Ed.* **2019**, *58*, 2844–2849; *Angew. Chem.* **2019**, *131*, 2870–2875; c) D. Mutruc, A. Goulet-Hanssens, S. Fairman, S. Wahl, A. Zimathies, C. Knie, S. Hecht, *Angew. Chem. Int. Ed.* **2019**, *58*, 12862–12867; *Angew. Chem.* **2019**, *131*, 12994–12999.

COMMUNICATION

Entry for the Table of Contents

